Journal of Alloys and Compounds 504 (2010) L1–L4

Contents lists available at ScienceDirect

Journal of Alloys and Compounds

journal homepage: www.elsevier.com/locate/jallcom

Letter

Facile hydrothermal synthesis of novel ZnO nanocubes

Lijie Yu, Fengyu Qu*, Xiang Wu*

College of Chemistry and Chemical Engineering, Harbin Normal University, Harbin 150025, People's Republic of China

ARTICLE INFO

Article history:
Received 2 April 2010
Received in revised form 4 May 2010
Accepted 5 May 2010
Available online 20 May 2010

Keywords:
ZnO
Nanostructures
Cathodoluminescence

ABSTRACT

In this paper, we reported the synthesis of cubic ZnO nanostructures by a facile hydrothermal route at mild reaction temperature without the addition of any surfactant. The as-obtained ZnO nanocubes are well crystalline and with an average size of 200 nm. The dependence of morphologies on growth parameters was systematically investigated. Cathodoluminescence of as-grown ZnO nanocubes shows a strong ultraviolet emission and a poor blue emission peak at room temperature.

© 2010 Elsevier B.V. All rights reserved.

1. Introduction

As is known, the shape and size of nanomaterials tremendously affect their physical and chemical properties. Rationally synthesizing nanostructures with desired shapes is prerequisite for studying the relations between the morphology and final properties and further integrating them into various nanodevices as well. Great attention has been paid to nanostructures with cubic shapes due to their unique and novel optical, optoelectronic and magnetic properties. Nanocubes of several metals, oxides and ternary element compounds have been reported. For example, Yang and co-workers synthesized α-Fe_2O_3 nanocubes through a hydrothermal reaction of $FeCl_3$ at 140 °C and investigated their gas-sensing properties [1]. Li and Zhang synthesized $NaTaO_3$ nanocubes as high performance photocatalysts by an aqueous approach [2]. Ge et al. studied on the origin of ferromagnetism in CeO_2 nanocubes [3]. Liang and co-workers synthesized catalytically active shape selective rhodium nanocubes with the assistant of organic surfactant [4]. Lupan et al. synthesized tetragonal SnO_2 microcubes and also investigated their possible growth mechanism [5]. Wang et al. synthesized hollow Cu_2O nanocubes and investigated their photocatalytic properties [6]. However, till now, only a few studies have been reported on ZnO nanocubes [7], and organic salts, such as sodium dioctyl sulfosuccinate, are usually required to get ZnO nanocubes.

ZnO is an important II–VI group semiconductor with a direct band gap energy of 3.37 eV and exciton binding energy of 60 meV at room temperature. ZnO owns the richest morphologies among all reported nanomaterials. Researchers intensively focusing on ZnO nanostructures are because of its three distinct properties, namely, semiconducting, piezoelectronic and biocompatible properties. So far, ZnO nanobelts [8,9], nanorods [10–12], nanotowers [13], nanorings [14,15], hollow nanoparticles [16], nanosprings [17,18], nanotubes [19–21], microspindles [22], and hierarchical heterostructures [23–26] have been synthesized by several growth methods. Among the synthetic methods, one-pot hydrothermal approach is a promising method since it is efficient, cost-effective and easy to manipulate. In this paper, we reported the synthesis of ZnO nanocubes grown at a mild temperature by a facile hydrothermal route without the assistant of any templates and surfactants. The effects of growth parameters on morphologies were investigated. A growth mechanism of the ZnO nanocubes was proposed. The cathodoluminescence results indicate the potential applications in ultraviolet or blue light emitting.

2. Experimental

All reagents are of analytical grade and used without further purification. In a typical procedure, 0.1 mol $Zn(NO_3)_2$ with the same mole amount of KOH was mixed and dissolved into 25 ml de-ionized water. The solution was stirred continuously until a transparent one was obtained. The solution and a pre-treated glass slice as the substrate were then sealed into a Teflon-lined autoclave, followed by hydrothermal reaction at 100 °C for 12 h. After that, the autoclave was naturally cooled to room temperature. The glass slice was taken out and washed several times with de-ionized water and ethanol, and dried at 100 °C for 6 h.

As-obtained product was characterized by X-ray diffraction (XRD, Rigaku Dmax-rB, Cu Kα radiation, $\lambda = 0.1542$ nm 40 kV, 100 mA), scanning electron microscopy (SEM, Hatachi-4800), Raman spectroscopy (HR800), and transmission electron microscopy (TEM, JEOL JEM-3000F). The samples for TEM were prepared by dispersing the synthesized ZnO product on a carbon-coated copper grid. Cathodoluminescence properties are investigated by means of a thermal field emission scanning electron microscope (Hitachi S4200) equipped with a CL system. The CL spectra and images are taken at room temperature at 15 kV and 500 pA.

---

* Corresponding authors. Fax: +86 451 88060653.
E-mail addresses: qufengyu@hrbnu.edu.cn (F. Qu), wuxiang05@gmail.com (X. Wu).

0925-8388/$ – see front matter © 2010 Elsevier B.V. All rights reserved.
doi:10.1016/j.jallcom.2010.05.055

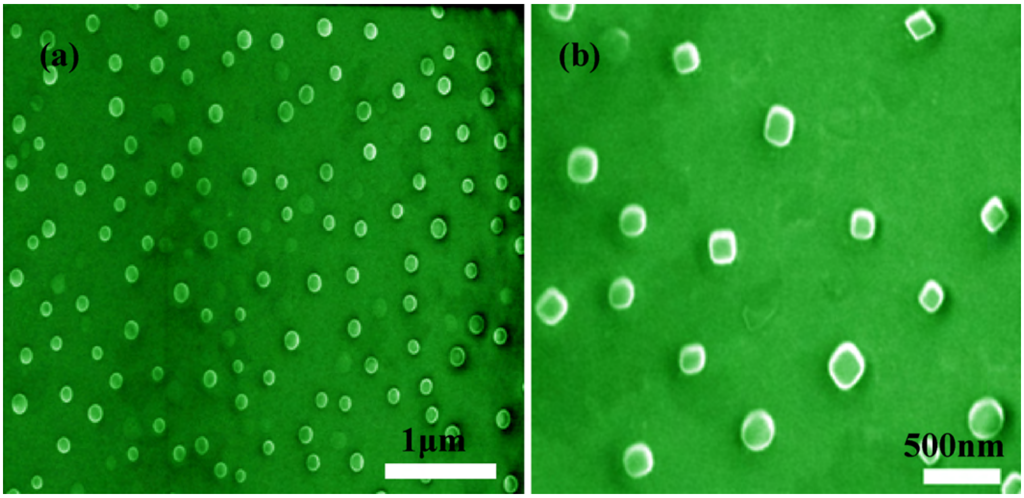

Fig. 1. SEM images of as-grown ZnO nanocubes: (a) low magnification images and (b) high magnification images.

3. Results and discussion

First, we utilized SEM to observe the morphologies of as-obtained product. Fig. 1a was a general SEM image of a synthesized nanostructure, from which large quantity of well-dispersed particle-shaped products lying on the glass substrate can be clearly seen. Further observation at high magnification found that most of the particles presented cubic shapes, namely, nanocubes, as shown in Fig. 1b. These nanocubes have the sizes ranging from 180 nm to 230 nm with an average size of about 200 nm. EDS spectrum (not shown here) indicated that only Zn and O elements appear without other impurity, which means as-obtained nanocubes are ZnO with high purity.

Raman spectrum was used to analyze the vibration states of as-synthesized ZnO nanocubes. Five Raman peaks located at 292 cm^{-1}, 335 cm^{-1}, 403 cm^{-1}, 438 cm^{-1} and 534 cm^{-1}, respectively, are clearly seen as shown in Fig. 2. ZnO with wurtzite crystal structure belongs to the C_{6v} space group with the two formula units per primitive cell and all the atoms occupying the C_{3v} symmetry. Near the center of the Brillouin zone, the group theory predicts the existence of the different optic modes. Raman active modes for the wurtzite ZnO are: $\Gamma = A_1 + 2E_2 + E_1$, where the A_1, E_1, and $2E_2$ modes are Raman active and split into longitudinal (LO) and transverse (TO) optical components [13,27,28]. The peak at 438 cm^{-1} in Fig. 2 was assigned as the optical phonon E_2, which corresponds to the band characteristic of ZnO wurtzite hexagonal phase [25]. Peaks located at 335 cm^{-1} and 534 cm^{-1} correspond to polar transverse A_1 and longitudinal E_1 optical phonon modes, respectively. The suppressed E_2 peak means the as-obtained ZnO nanocubes own large structure defects such as oxygen vacancies.

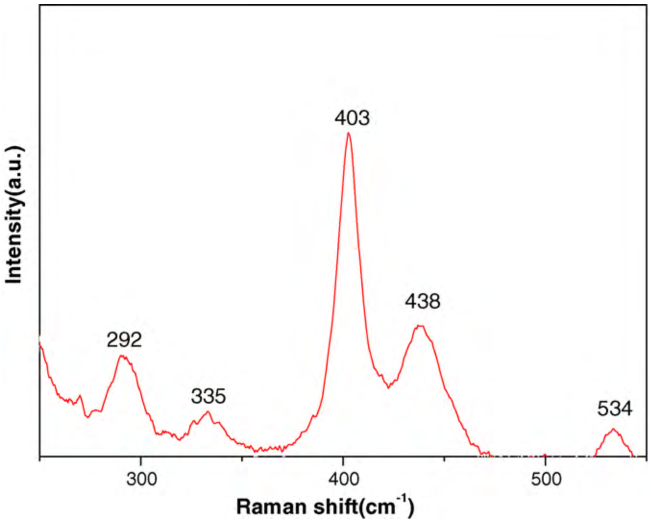

Fig. 2. Raman spectrum of as-grown ZnO nanocubes.

TEM is employed to study the microstructural characteristics of as-obtained ZnO nanocubes in detail, and the results are given in Fig. 3. Fig. 3a is a typical low magnification TEM image of an individual nanocube. The size of the nanocube is about 200 nm. Interestingly, irregular fringes are found located at each edge of the nanocube. Fig. 3b is a HRTEM image taken from the rectangular mark in Fig. 3a. The measured *d* value is 0.26 nm, which is consistent with the (0 0 0 2) plane of wurtzite ZnO phase. The inset in Fig. 3b is the corresponding FFT pattern, which is in agreement with the HRTEM result.

To get further insight into the formation mechanism of as-obtained ZnO nanocubes, temperature and organic additives dependent morphology evolution were performed. When the reaction temperature was lower than 90 °C and the other growth parameters kept constant, no nanocubes were found and only plentiful sphere-like nanoparticles appeared. As-synthesized nanoparticles are 80–240 nm in size, as shown in Fig. 4a and b. When 0.05 mol hexamethylenetetramine (HMT) was added into the above solution and reaction temperature kept unchanged at 100 °C, only some nanocrystals with large size variation sparsely dispersed on the glass substrate (Fig. 4c and d) instead of nanocubes shown in Fig. 1. The above results indicated that tailoring the growth parameters is an efficient way to obtain desired nanostructures.

Based on the above-mentioned experimental results, a possible growth mechanism of the ZnO nanocubes can be proposed as follows: from the crystallization point of view, the formation of the nanostructures is expected to experience a nucleation and growth process during hydrothermal reaction. At first stage, Zn^{2+} and OH^- from the hydrolysis of $Zn(NO_3)_2$ and KOH reacted with each other to form $Zn(OH)_2$. With the on-going of chemical reaction, the nucleation and crystal growth rate would be higher. The amphoteric $Zn(OH)_2$ reacted with OH^- and created more ZnO^{2-} nuclei. Then these newly formed ZnO^{2-} nuclei interacted with water molecules and can be fused small ZnO particles due to kinetic process of crystal growth. At elevated temperature, ZnO nanocubes were finally formed due to interaction among different growth direction with

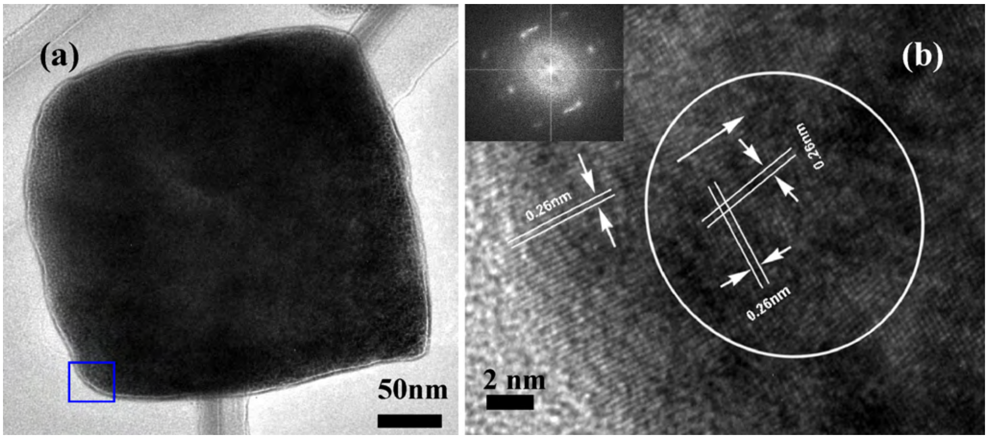

Fig. 3. TEM images of as-grown ZnO nanocubes: (a) low magnification image of a nanocube and (b) HRTEM image taken from the rectangular region; the inset is the corresponding FFT pattern.

different growth ratio. This explanation is in consistent with the growth of SnO_2 microcubes reported by Lupan et al. [5].

Finally, cathodoluminescence properties of as-grown ZnO nanocubes were studied at room temperature. Fig. 5 illustrated a cathodoluminescence spectrum taken at 15 kV, which showed a strong ultraviolet emission peak located at 374 nm and a slightly weak blue emission peak at 489 nm. Usually, the near band edge (NBE) emission of ZnO powder is located at 380 nm, which originates from the direct recombination of the free excitons through an exciton–exciton collision process. The ZnO nanocubes reported here have a strong UV emission peak at 374 nm, which shows a blue shift of about 6 nm in comparison with that of ZnO bulk material. The origins of visible luminescence of ZnO has been debated for many years. Recently, Zeng et al. systemically studied the blue photoluminescence of ZnO and proposed it originates from interstitial zinc defects [29]. The obvious blue luminescence and suppressed E_2 vibration mode indicate that there could be abundant lattice defects in the nanocubes, which could be the cause of the blue

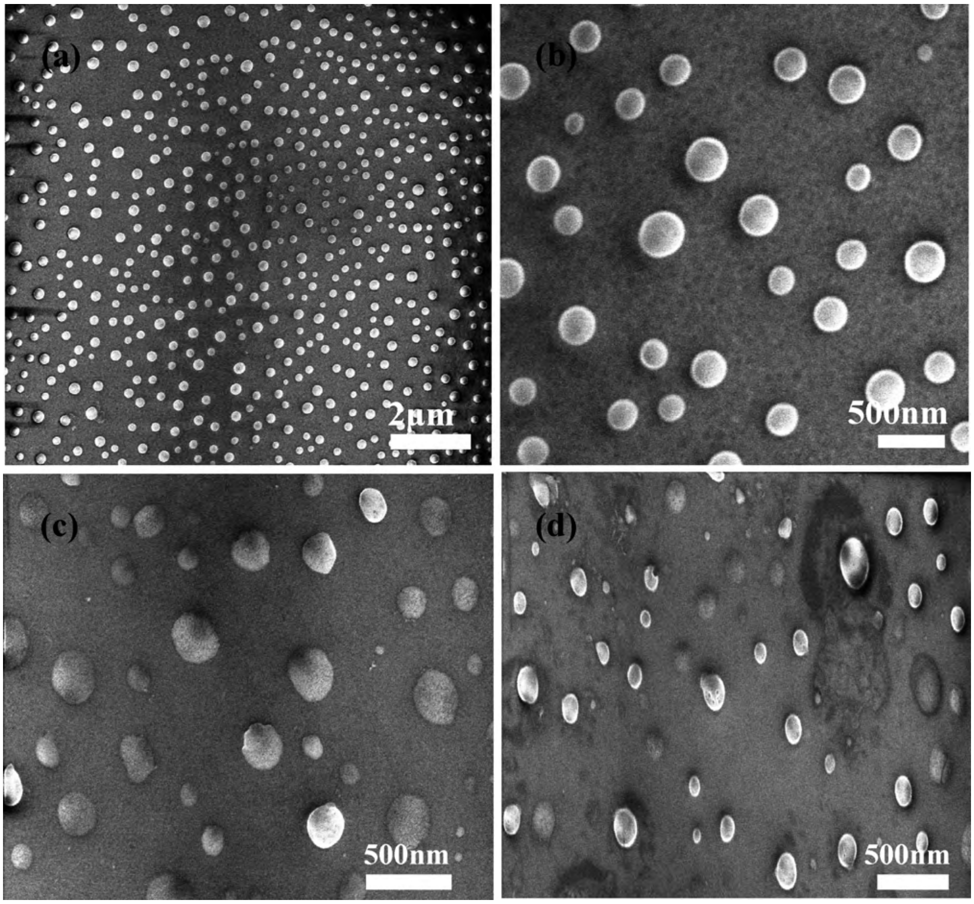

Fig. 4. SEM images of as-synthesized products in the different growth condition: (a) 0.1 mol $Zn(NO_3)$ with equal quantity KOH, at 90 °C temperature, (b) the corresponding high magnification images in (a), (c) 0.05 mol $Zn(NO_3)$ with equal quantity KOH, at 100 °C temperature with addition of 0.05 mol HMT and (d) the corresponding high magnification images in (c).

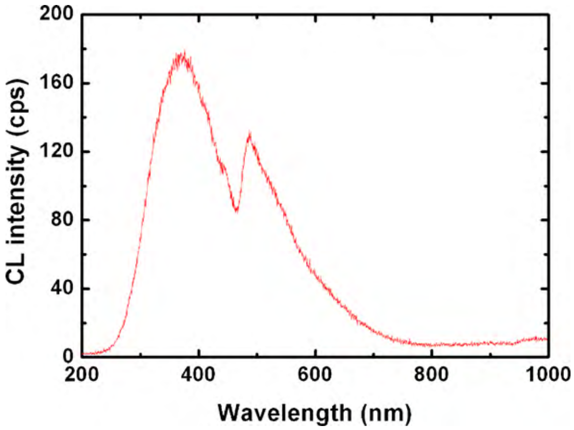

Fig. 5. CL spectrum of as-grown nanocubes at an accelerate voltage of 15 kV.

shift of UV emission in CL spectrum. These results indicated that as-synthesized ZnO nanocubes here may have potential applications in fabrication of optical and optoelectronic nanodevices.

4. Conclusions

In summary, we have successfully synthesized novel ZnO nanocubes through a facile hydrothermal approach at mild temperature. SEM images indicated that as-synthesized ZnO structures own a cuboid shape with an average size of 200 nm. The temperature and surfactant play important roles in shape evolution of the final products. A possible growth mechanism is proposed based on the experimental phenomenon. Cathodoluminescence properties of as-grown ZnO nanocubes at room temperature showed a strong ultraviolet emission peak located at 374 nm and a poor blue emission peak at 489 nm, which mean to be applicable in fabrication of optical and optoelectronic nanodevices.

Acknowledgements

This work was supported by the Doctor Start-up Fund of Harbin Normal University (KGB200802), the National Natural Science Foundation of China (20871037), the Natural Science Foundation of Heilongjiang Province (B2007-2) and the Science Technology and Research Project of Education Bureau, Heilongjiang Province (11531229). Dr. Benjamin Dierre is thanked for his kind help in CL test.

References

[1] F.H. Zhang, H.Q. Yang, X.L. Xie, L. Li, L.H. Zhang, J. Yu, H. Zhao, B. Liu, Sens. Actuators B 141 (2009) 381.

[2] X. Li, J.L. Zhang, J. Phys. Chem. C 113 (2009) 19411.

[3] M.Y. Ge, H. Wang, E.Z. Liu, J.F. Liu, J.Z. Jiang, Y.K. Li, Z.A. Xu, H.Y. Li, Appl. Phys. Lett. 93 (2008) 062505.

[4] S. Kundu, K. Wang, H. Liang, J. Phys. Chem. C 113 (2009) 18570.

[5] O. Lupan, L. Chowa, G. Chai, H. Heinrich, S. Park, A. Schulte, J. Cryst. Growth 311 (2008) 152.

[6] Z.H. Wang, H. Wang, L.L. Wang, L. Pan, J. Phys. Chem. Solids 70 (2009) 719.

[7] P. Gao, Y.J. Chen, Y. Wang, Q. Zhang, X.F. Li, M. Hu, Chem. Commun. (2009) 2762.

[8] Z.W. Pan, Z.R. Dai, Z.L. Wang, Science 291 (2001) 1897.

[9] P.G. Li, S.L. Wang, W.H. Tang, J. Alloys Compd. 489 (2010) 566.

[10] Q. Ahsanulhaq, S.H. Kim, Y.B. Hahn, J. Alloys Compd. 484 (2009) 17.

[11] G.Z. Shen, Y. Bando, B.D. Liu, C.Y. Zhi, D. Golberg, J. Phys. Chem. B 110 (2006) 3973.

[12] H.B. Zeng, X.J. Xu, Y. Bando, U.K. Gautam, T.Y. Zhai, X.S. Fang, B.D. Liu, D. Golberg, Adv. Funct. Mater. 19 (2009) 3165.

[13] X. Wu, P. Jiang, W. Cai, X.D. Bai, P. Gao, S.S. Xie, Adv. Eng. Mater. 10 (2008) 476.

[14] X.Y. Kong, Y. Ding, R.S. Yang, Z.L. Wang, Science 303 (2004) 1348.

[15] X. Wu, F.Y. Qu, X. Zhang, W. Cai, G.Z. Shen, J. Alloys Compd. 486 (2009) L13.

[16] H.B. Zeng, W.P. Cai, P.S. Liu, X.X. Xu, H.J. Zhou, C. Klingshirn, H. Kalt, ACS Nano 2 (2008) 1661.

[17] P.X. Gao, Z.L. Wang, Small 1 (2005) 945.

[18] X. Wu, W. Cai, F.Y. Qu, Chin. Phys. B 18 (2009) 1669.

[19] H.B. Chen, X. Wu, L.H. Gong, C. Ye, F.Y. Qu, G.Z. Shen, Nanoscale Res. Lett. 5 (2010) 570.

[20] J.S. Jeong, J.Y. Lee, J.H. Cho, H.J. Suh, C.J. Lee, Chem. Mater. 17 (2005) 2752.

[21] L. Li, S.S. Pan, X.C. Dou, Y.G. Zhu, X.H. Huang, Y.W. Yang, G.H. Li, L.D. Zhang, J. Phys. Chem. C 111 (2007) 7288.

[22] L.H. Gong, X. Wu, C. Ye, F.Y. Qu, M.Z. An, J. Alloys Compd. 501 (2010) 375.

[23] X. Wu, P. Jiang, Y. Ding, W. Cai, S.S. Xie, Z.L. Wang, Adv. Mater. 19 (2007) 2319.

[24] G.Z. Shen, D. Chen, C.J. Lee, J. Phys. Chem. B 110 (2006) 15689.

[25] J. Yan, X.S. Fang, L.D. Zhang, Y. Bando, U.K. Gautam, B. Dierre, T. Sekiguchi, D. Golberg, Nano Lett. 8 (2008) 2794.

[26] X.S. Fang, Y. Bando, U.K. Gautam, T.Y. Zhai, H.B. Zeng, X.J. Xu, M.Y. Liao, D. Golberg, Crit. Rev. Solid State Mater. Sci. 34 (2009) 190.

[27] A. Umar, S.H. Kim, Y.S. Lee, K.S. Nahm, Y.B. Hahn, J. Cryst. Growth 282 (2005) 131.

[28] T.C. Damen, S.P.S. Porto, B. Tell, Phys. Rev. 142 (1966) 570.

[29] H.B. Zeng, G.T. Duan, Y. Li, S.K. Yang, X.X. Xu, W.P. Cai, Adv. Funct. Mater. 20 (2010) 561.